Dielectronic recombination for C V, VI and O VII, VIII

R. Bellantone and Yukap Hahn
Department of Physics, University of Connecticut, Storrs, Connecticut 06269
(Received 9 May 1989)

Dielectronic recombination (DR) cross sections and rate coefficients for the H-like and He-like C and O ions are calculated in the zero-field, zero-density limit. The peak rates are approximately $(1.2-1.6)\times10^{-12}$ cm^3/sec for all four ions. For the H-like ions, the contribution to total rates from high Rydberg states ($n \geq 6$) is found large, accounting for nearly one-half of the total rates. Agreements with earlier estimates are at a $\pm5\%$ level. For the He-like ions, the high-Rydberg-state contribution is strongly suppressed because of the extra Auger channel which opens up at $n=5-7$. Agreement with previous calculations is again at a 5% level. The DR cross sections for the initial metastable states of the He-like ions are also estimated for a few low-lying resonance states near the DR threshold. The cross section for the $2s\,{}^1S \rightarrow 1s2p\,{}^1P + nl$ excitation capture is found to be very large.

I. INTRODUCTION

Radiative cooling of magnetically confined plasmas with heavy impurity ions was a serious obstacle in attaining high temperature. Radiations are emitted by excited ions produced by collisional excitation and electron capture, and heavy impurity ions are efficient x-ray emitters, via the resonant capture process, the dielectronic recombination (DR). Many of the heavy elements in early tokamak plasmas are now eliminated, but there are sizable amounts of C and O ions still present. The carbon ions are produced during a meltdown of the carbon lim-

TABLE I. DR cross sections, in units of 10^{-20} cm^2 and $\Delta e_c = 1$ Ry, and rate coefficients, in units of 10^{-13} cm^3/sec, are given for C^{5+}, where the electron temperature $k_B T_e$ is given in rydbergs.

d	e_c (Ry)	$\bar{\sigma}$ (10^{-20} cm^2)	DR rates (10^{-13} cm^3/sec) $kT=5.5$ Ry	$kT=11$ Ry	$kT=22$ Ry	$kT=44$ Ry
$2s2p$	21.41	0.321	0.268	0.664	0.628	0.357
$2p^2$	21.99	0.262	0.107	0.528	0.507	0.296
$2s3p$	24.99	0.0661	0.0336	0.115	0.127	0.0790
$2p3s$	23.98	0.222	0.130	0.407	0.428	0.261
$2p3p$	24.03	0.209	0.135	0.422	0.444	0.271
$2p3d$	25.25	0.545	0.267	0.936	1.043	0.655
$2s4p$	25.93	0.0252	0.0112	0.0417	0.0479	0.0305
$2p4s$	25.34	0.161	0.0780	0.276	0.309	0.194
$2p4p$	25.37	0.181	0.0868	0.308	0.345	0.217
$2p4d$	25.41	0.465	0.223	0.792	0.888	0.560
$2p4f$	25.44	0.115	0.0549	0.196	0.220	0.139
$3s3p$	29.43	0.0009	0.0026	0.0013	0.0018	0.0012
$3p^2$	29.59	0.0030	0.0008	0.0041	0.0056	0.0039
$3p3d$	29.69	0.0293	0.0086	0.0453	0.0618	0.0429
$2p5s$	25.95	0.119	0.0527	0.197	0.226	0.145
$2p5p$	25.96	0.162	0.0718	0.269	0.312	0.198
$2p5d$	25.99	0.373	0.165	0.618	0.713	0.454
$2p5f$	26.00	0.093	0.0407	0.153	0.176	0.113
$2p5g$	26.00	0.0025	0.00112	0.0042	0.0048	0.0031
$2pns$, $n \geq 6$		0.585	0.258	0.968	1.113	0.712
$2pnp$		1.658	0.732	2.753	3.166	2.025
$2pnd$		1.608	0.708	2.660	3.059	1.957
$2pnf$		0.238	0.105	0.394	0.453	0.290
$2png$		0.006	0.0026	0.0098	0.0113	0.0072
Others		0.15	0.08	0.26	0.28	0.18
Total			3.62	13.0	14.6	9.19

iter by edge plasmas, and the oxygen ions are present mainly due to the outgasing of container walls. For plasma temperatures in the keV range attainable by current tokamaks, C^{Z+} and O^{Z+} are found in all charge states, $Z < Z_c$ where Z_c is the nuclear core charge. The modeling of such plasmas therefore requires reaction rates for the complete set of ionization states, with an accuracy of $\pm 20\%$ or better.

In this paper, we evaluate explicitly the DR cross sections and rate coefficients for the H-like and He-like C and O ions, with the number of electrons N in the initial ions being $N=1$ and 2. Approximations introduced are explicitly spelled out. Our results are then compared with several previous calculations. A careful assessment of the accuracy of the existing data for these ions is made.

In addition, we also estimated the DR cross sections for low-lying resonance states produced from the initial ions in the metastable states in O^{6+}. The $1s2s$ singlet $\rightarrow 1s2p$ singlet excitation capture transitions was found dominant with an unusually large cross section.

II. THEORETICAL PROCEDURE

As is well known, DR is a resonant electron-ion collision process[1] involving two or more electrons, and the theoretical treatment of such many-body problems requires many simplifying approximations. In order to be able to assess the reliability of the calculation, it is important to carefully specify the approximations introduced. The present work follows the standard procedure[2] which involves the following approximations, most of which are proven to be adequate in producing data for plasma modeling applications.

(i) All the ionic bound state orbitals used in the evaluation of the Auger and radiative transition probabilities A_a and A_r are generated by the nonrelativistic Hartree-Fock procedure (NRHF). The spin-orbit interaction and other relativistic corrections are neglected, but can be included perturbatively, if necessary, so long as the core charge Z_c is not too large ($Z_c < 40$).

(ii) The continuum orbitals needed for A_a are calculated in the single-channel distorted-wave method using the NRHF potential, both for the direct and exchange (nonlocal) interactions. Possible dispersion and absorption effects have been omitted; they may be included by an effective (optical) potential method, as these effects are especially important in the treatment of ionization and excitation processes.

(iii) The single-configuration approximation is adopted throughout. As is well known, this can often lead to grossly erroneous results for those individual radiative and Auger transitions with small transition probabilities. However, for total rates and cross-section sums, the configuration interaction effect often averages out. Some

TABLE II. DR cross sections, in units of 10^{-20} cm^2 and $\Delta e_c = 1$ Ry, and rate coefficients, in units of 10^{-13} cm^3/sec, are given for O^{7+}, where the electron temperature $k_B T_e$ is given in rydbergs.

			DR rates (10^{-13} cm^3/sec)			
d	e_c (Ry)	$\bar{\sigma}$ (10^{-20} cm^2)	$kT=10.35$ Ry	$kT=20.7$ Ry	$kT=41.4$ Ry	$kT=82.8$ Ry
$2s2p$	36.59	0.530	0.417	0.864	0.739	0.407
$2p^2$	37.38	0.495	0.369	0.794	0.692	0.385
$2s3p$	43.59	0.113	0.0540	0.157	0.159	0.0953
$2p3s$	42.21	0.293	0.155	0.420	0.412	0.242
$2p3p$	42.29	0.352	0.185	0.504	0.495	0.292
$2p3d$	43.97	0.739	0.343	1.015	1.038	0.624
$2s4p$	45.61	0.0430	0.0177	0.0567	0.0603	0.0370
$2p4s$	44.80	0.180	0.0786	0.242	0.252	0.153
$2p4p$	44.83	0.320	0.123	0.379	0.395	0.240
$2p4d$	44.90	0.571	0.248	0.767	0.802	0.488
$2p4f$	44.93	0.0960	0.0417	0.129	0.135	0.0822
$3s3p$	51.71	0.0016	0.0004	0.0018	0.0022	0.0014
$3p^2$	51.92	0.0053	0.0014	0.0059	0.0073	0.0048
$3p3d$	52.06	0.0416	0.0105	0.0458	0.0572	0.0379
$2p5s$	45.97	0.124	0.0498	0.162	0.174	0.107
$2p5p$	45.99	0.237	0.0944	0.308	0.331	0.204
$2p5d$	46.02	0.411	0.164	0.536	0.576	0.355
$2p5f$	46.04	0.0754	0.0301	0.0982	0.106	0.0651
$2p5g$	46.04	0.00211	0.0008	0.00275	0.0030	0.0018
$2pns$, $n \geq 6$		0.468	0.187	0.612	0.657	0.406
$2pnp$		1.672	0.665	2.172	2.328	1.439
$2pnd$		1.330	0.531	1.734	1.862	1.149
$2pnf$		0.187	0.0747	0.244	0.262	0.162
$2png$		0.0043	0.0017	0.0057	0.0061	0.0038
Others		0.30	0.08	0.24	0.26	0.18
Total			3.92	11.5	11.8	7.16

test calculations are usually carried out to ascertain this problem.

(iv) For light ions with $Z < 20$, the LS coupling procedure is found to be adequate. For systems with more than two electrons, however, there are several different ways by which electrons are coupled in pairs. The simplest is the active-electron-pair coupling (APC) which we adopted in this and all the earlier work. The angular momentum recoupling is minimal in APC, as the electronic states which are directly involved in a given transition are first coupled, followed by the coupling of all the other spectator electrons. Another common alternative is the core-electron sequential coupling (CSC) in which the innermost-shell electrons are coupled first, and one gradually works his way to outer-shell electrons. Configuration mixing and/or intermediate coupling rectify to some extent this dependence of the calculated rates on the coupling order.

(v) As noted, DR is a resonant process and in general there are many resonance levels which contribute in a given energy bin Δe_c; some levels strongly overlap with each other, especially for those resonance states involving high-Rydberg-state electrons. The simplest procedure here is the isolated resonance approximation in which each resonant state is treated separately from all the other states which lie nearby. The effect of overlapping resonances is usually small for low-lying states, but can be sizable for high Rydberg states (HRS) near the ionization threshold. (The states near the threshold have to be treated with care, since they are spatially very large, and can be severely distorted by experimental conditions, such as stray electric fields and the presence of other charged particles nearby.)

(vi) The radiative cascade effect is important and has to be properly incorporated. That is, some radiative transitions in the decay of the primary resonance states may lead to final states which are not Auger stable. This will decrease the overall DR rates. An example of this is the decay of $1s2p3d \rightarrow 1s2p^2+\gamma$, where the $1s2p^2$ $(S=\frac{1}{2})$ state is Auger unstable. Thus contribution of the A_r for the above process to fluorescence yield has to be reduced by the branching ratio $(\omega < 1)$ of the $1s2p^2$ state, although it does not affect the full width of the original $1s2p3d$ state.

(vii) For given intermediate state (d), there can be more than one Auger channel allowed by energy, angular momentum, and parity conservations. That is, $\Gamma_a(d)=\sum_{i'} A_a(d \rightarrow i')$, where i' includes the initial state, as well as other Auger channels. In particular, there can be Auger channels of the $\Delta n_t = 0$ type in which the corresponding A_a can be very large. An example is $1s2pnd \rightarrow 1s2s+e'$, where $n \geq n_m = 7$ for O^{6+}. The presence of such channels can drastically reduce the cross section and rate coefficients.[3]

(viii) The HRS (nl) contributions are estimated using the n-scaling behavior of A_a and A_r for n sufficiently large $(n \gtrsim 3l)$. It is important to keep in mind, however, that extrapolation to high-n states by n scaling must be carried out first for the individual A's, noting that some of the A's can be n independent.[1] Attempts to scale directly the cross sections or the rates can often lead to a

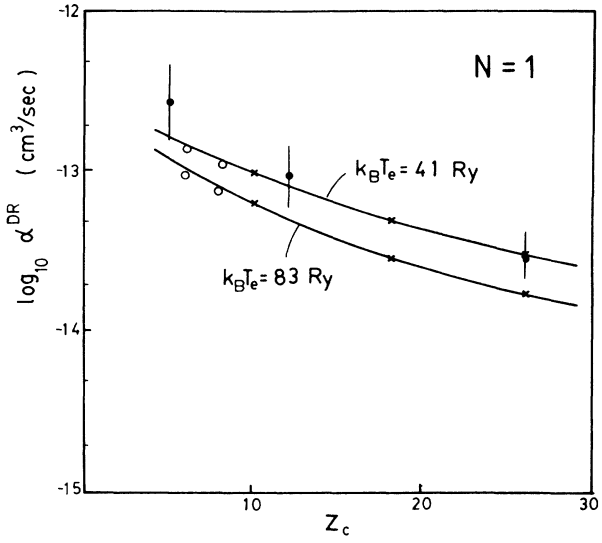

FIG. 1. Comparison of the DR rates for C^{5+} and O^{7+} with the extrapolated data from earlier studies, Refs. 5 and 6. The open circles are the result of this calculation. The high-Z_c results (solid curves and ×) are from the theoretical calculation of Ref. 5, and some earlier estimate from Ref. 6 (●) is also indicated.

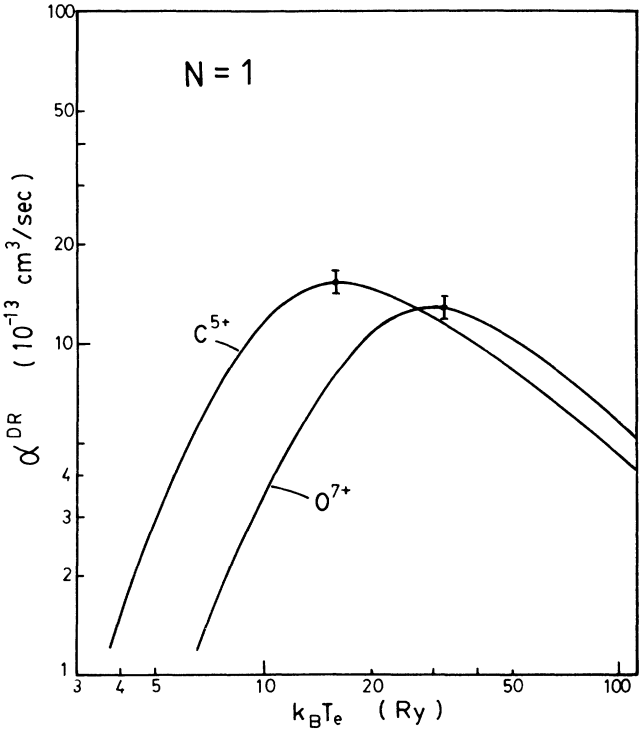

FIG. 2. DR rates for C^{5+} and O^{7+}, in units of 10^{-13} cm^3/sec, are given as functions of electron temperature k_BT_e, in rydbergs. An estimated accuracy of ±5% of the calculation is indicated.

TABLE III. DR cross sections and rate coefficients are given for C^{4+}. The state-by-state contributions are tabulated for all the dominant intermediate states. The high-Rydberg-state contribution is given separately for $n \geq 5$. All the Auger channels are open for $n \geq 6$, where the n^{-3} scaling properties of the transition probabilities involving HRS electrons are used to extrapolate the cross sections and rates. The DR rates are given in units of cm^3/sec, and the cross sections in units of cm^2 for $\Delta e_c = 1$ Ry. The electron temperature is given in the parentheses following α, in rydbergs. The extrapolated value for $|1s2s4p\rangle$, for example, contains all np states with $n \geq 5$ but excluding $4p$.

$\|1d\rangle$	L_{ab}	S_{ab}	e_c (Ry)	α (5.77)	α (22.07)	α (73.55)	$\bar{\sigma}$
$\|1s2s2p\rangle$	1	0	17.12	1.52×10^{-14}	1.82×10^{-14}	5.14×10^{-15}	9.69×10^{-22}
	1	1	17.12	4.50×10^{-14}	5.39×10^{-14}	1.52×10^{-14}	2.87×10^{-21}
$\|1s2s3p\rangle$	1	0	20.04	2.11×10^{-15}	3.67×10^{-15}	1.14×10^{-15}	1.91×10^{-22}
	1	1	20.04	6.26×10^{-15}	1.09×10^{-14}	3.38×10^{-15}	5.65×10^{-22}
$\|1s2s4p\rangle$	1	0	20.92	7.27×10^{-16}	1.41×10^{-15}	4.51×10^{-16}	7.32×10^{-23}
	1	1	20.92	2.16×10^{-15}	4.19×10^{-15}	1.34×10^{-15}	2.17×10^{-22}
$\|1s2p2\rangle$	0	0	17.71	9.05×10^{-15}	1.17×10^{-14}	3.36×10^{-15}	6.18×10^{-22}
	2	0	17.71	4.55×10^{-14}	5.87×10^{-14}	1.69×10^{-14}	3.10×10^{-21}
$\|1s2p3s\rangle$	1	0	20.29	8.86×10^{-15}	1.59×10^{-14}	4.97×10^{-15}	8.25×10^{-22}
	1	1	20.29	2.47×10^{-14}	4.43×10^{-14}	1.39×10^{-14}	2.30×10^{-21}
$\|1s2p3p\rangle$	0	0	20.42	3.35×10^{-15}	6.11×10^{-15}	1.92×10^{-15}	3.17×10^{-22}
	0	1	20.42	2.14×10^{-15}	3.90×10^{-15}	1.22×10^{-15}	2.02×10^{-22}
	2	0	20.42	1.69×10^{-14}	3.08×10^{-14}	9.66×10^{-15}	1.60×10^{-21}
	2	1	20.42	8.76×10^{-15}	1.60×10^{-14}	5.02×10^{-15}	8.29×10^{-22}
$\|1s2p3d\rangle$	1	0	20.54	1.03×10^{-15}	1.91×10^{-15}	6.03×10^{-16}	9.92×10^{-23}
	1	1	20.54	5.97×10^{-15}	1.11×10^{-14}	3.49×10^{-15}	5.73×10^{-22}
	3	0	20.54	1.88×10^{-14}	3.49×10^{-14}	1.10×10^{-14}	1.81×10^{-21}
	3	1	20.54	4.74×10^{-14}	8.78×10^{-14}	2.77×10^{-14}	4.55×10^{-21}
$\|1s2s4p\rangle$			20.92	2.88×10^{-15}	5.61×10^{-15}	1.79×10^{-15}	2.91×10^{-22}
$\|1s2p4s\rangle$			21.24	2.53×10^{-14}	5.12×10^{-14}	1.65×10^{-14}	2.65×10^{-21}
$\|1s2p4p\rangle$			21.30	2.18×10^{-14}	4.45×10^{-14}	1.44×10^{-14}	2.30×10^{-21}
$\|1s2p4d\rangle$			21.34	5.40×10^{-14}	1.11×10^{-13}	3.59×10^{-14}	5.74×10^{-21}
$\|1s2p4f\rangle$			21.36	9.61×10^{-15}	1.98×10^{-14}	6.40×10^{-15}	1.02×10^{-21}
$\|1s2p5s\rangle$			21.66	1.98×10^{-14}	4.24×10^{-14}	1.39×10^{-14}	2.20×10^{-21}
$\|1s2p5p\rangle$			21.69	1.77×10^{-14}	3.79×10^{-14}	1.24×10^{-14}	1.96×10^{-21}
$\|1s2p5d\rangle$			21.71	6.68×10^{-16}	1.44×10^{-15}	4.70×10^{-16}	7.43×10^{-23}
$\|1s2p5f\rangle$			21.72	3.83×10^{-17}	8.25×10^{-17}	2.70×10^{-17}	4.27×10^{-24}
Totals				4.13×10^{-13}	7.24×10^{-13}	2.26×10^{-13}	3.77×10^{-13}

				Extrapolation values using scaling			
Extrapolated from $\|d\rangle$	L_{ab}	S_{ab}	e_c (Ry)	α (5.77)	α (22.07)	α (73.55)	$\bar{\sigma}$
$\|1s2s4p\rangle$	1	0	20.92	1.01×10^{-15}	2.14×10^{-15}	6.98×10^{-16}	1.11×10^{-22}
	1	1	20.92	3.01×10^{-15}	6.36×10^{-15}	2.07×10^{-15}	3.29×10^{-22}
$\|1s2p5s\rangle$	1	0	21.66	3.82×10^{-15}	8.86×10^{-15}	2.95×10^{-15}	4.58×10^{-22}
	1	1	21.66	1.71×10^{-14}	3.92×10^{-14}	1.30×10^{-14}	2.03×10^{-21}
$\|1s2p5p\rangle$	0	0	21.69	1.67×10^{-15}	3.88×10^{-15}	1.29×10^{-15}	2.00×10^{-22}
	0	1	21.69	1.03×10^{-16}	2.39×10^{-16}	7.97×10^{-17}	1.24×10^{-23}
	2	0	21.69	1.26×10^{-13}	2.91×10^{-13}	9.69×10^{-14}	1.51×10^{-20}
	2	1	21.69	3.57×10^{-15}	8.12×10^{-15}	2.69×10^{-15}	4.20×10^{-22}
$\|1s2p5d\rangle$	1	0	21.71	2.25×10^{-17}	5.23×10^{-17}	1.75×10^{-17}	2.71×10^{-24}
	1	1	21.71	2.69×10^{-16}	6.23×10^{-16}	2.08×10^{-16}	3.22×10^{-23}
	3	0	21.71	2.87×10^{-15}	6.69×10^{-15}	2.23×10^{-15}	3.46×10^{-22}
	3	1	21.71	7.36×10^{-15}	1.70×10^{-14}	5.67×10^{-15}	8.81×10^{-22}
$\|1s2p5f\rangle$	2	0	21.72	8.90×10^{-18}	2.05×10^{-17}	6.80×10^{-18}	1.06×10^{-24}
	2	1	21.72	1.45×10^{-17}	3.31×10^{-17}	1.10×10^{-17}	1.71×10^{-24}
	4	0	21.72	1.30×10^{-16}	3.02×10^{-16}	1.01×10^{-16}	1.56×10^{-23}
	4	1	21.72	4.71×10^{-16}	1.09×10^{-15}	3.64×10^{-16}	5.65×10^{-23}
Total extrapolations				1.68×10^{-13}	3.86×10^{-13}	1.28×10^{-13}	2.00×10^{-20}

TABLE III. (*Continued*).

Extrapolated from $\|d\rangle$	L_{ab}	S_{ab}	e_c (Ry)	Extrapolation values using scaling α (5.77)	α (22.07)	α (73.55)	$\bar{\sigma}$
				Totals including extrapolation α (5.77)	α (22.07)	α (73.55)	σ
				5.81×10^{-13}	1.11×10^{-12}	3.55×10^{-13}	5.76×10^{-20}

gross underestimation of the HRS contributions. Also of importance is to make sure that all the allowed Auger channels are open for $n \geq n_m$, where the scaling estimate is made.

(ix) Finally, many of the energy levels used in the calculation have to be adjusted against better experimental values or those generated by Cowan's (RCN) code.[4] This adjustment has two important effects; (i) A_r is especially sensitive to the transition energies ($A_r \sim \hbar\omega_\gamma^3$), and (ii) the n_m values have to be determined using the correct threshold energies, so that all the Auger channels are properly included for those states with $n \geq n_m$. The expressions used for the cross section and rate coefficients are[1]

$$\bar{\sigma}^{\mathrm{DR}}(i)=\frac{4\pi}{\Delta e_c}\sum_d \frac{1}{e_c} V_a(i\rightarrow d)\omega_c(d)(\pi a_0^2) \tag{1}$$

and

$$\alpha^{\mathrm{DR}}(i)=\left[\frac{4\pi}{k_B T_e}\right]^{3/2}\sum_d V_a(i\rightarrow d)\omega_c(d)e^{-e_c/k_B T_e}, \tag{2}$$

where e_c is the kinetic energy of the incident electron, in rydbergs, which depends on the state d via the resonance condition, and

$$V_a(i\rightarrow d)=(g_d/2g_i)A_a(d\rightarrow i) \quad (\text{in sec}) \tag{3}$$

is the radiationless excitation-capture probability given in units of sec^{-1}, $k_B T_e$ is the plasma temperature, in rydbergs and $\omega_c(d)$ is the cascade corrected fluorescence yield,

$$\sum_f \omega(d\rightarrow f)+\sum_{f,d'}\omega(d\rightarrow d')\omega(d'\rightarrow f)+\cdots, \tag{4}$$

where the partial fluorescence yield

$$\omega(d\rightarrow d')=A_r(d\rightarrow d')/\Gamma(d), \tag{5}$$

where $\Gamma(d)=\Gamma_a+\Gamma_r$.

III. RESULTS

A. Hydrogen-like ions

We start with the H-like C^{5+} and O^{7+}. These are the simplest cases in which DR can take place, and no spectator electrons are present during the excitation capture. Tables I and II contain the details of our calculation, following the procedure outlined in Sec. II. The extrapolation from the data of Karim and Bhalla[5] is shown in Fig. 1, which indicates that our result is approximately 3–5 % lower, but the overall trend is well reproduced by the two calculations. From this comparison, we conclude that the DR rates for C VI and O VIII have now converged to within ±5%. Also indicated in Fig. 1 are some data from the compilation of Fujimoto *et al.* We note that, although only the $\Delta n_t \neq 0$ excitation transitions are involved here, i.e., $1s\rightarrow 2s$, $2p$, etc., the HRS contribution (for $n > 6$) is quite large, nearly 50% of the total. This is in sharp contrast with the He-like ions to be discussed below, and due mainly to the fact that the core states $2s$ and $2p$ of the inner electron in the intermediate-state configurations are nearly degenerate in the absence of any spectator electrons. Figure 2 summarizes the rates for C^{5+} and O^{7+}.

B. He-like ions

The He isoelectronic sequence is the most extensively studied case,[7–9] in particular for the low-lying states of

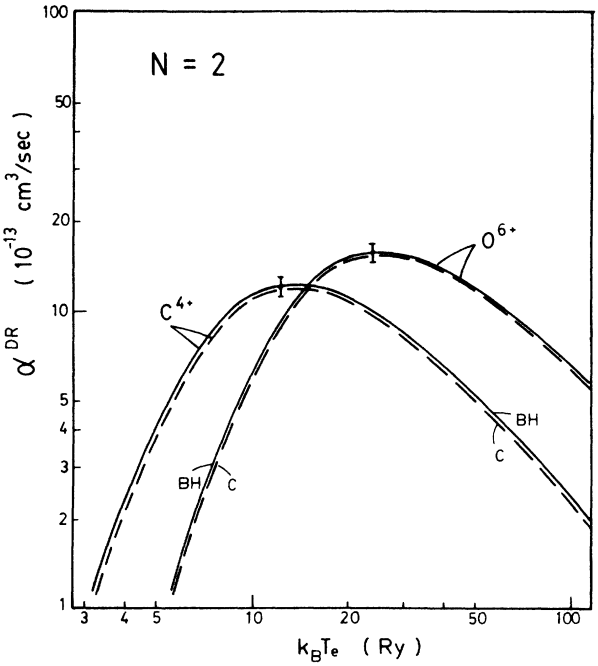

FIG. 3. DR rates for C^{4+} and O^{6+}, in units of 10^{-13} cm^3/sec, are given as functions of electron temperature $k_B T_e$ in rydbergs (solid curves). The earlier results from Ref. 12 are given in dashed curves. The estimated uncertainty of the calculation is also indicated.

TABLE IV. DR cross sections and rate coefficients are given for O^{6+}. The state-by-state contributions are tabulated for all the dominant intermediate states. The high-Rydberg-state contribution is given separately for $n < 7$. All the Auger channels are open at ≥ 7, but the scaling properties are used for ≥ 6. The units used are the same as those in Table III. The extrapolated value for $|1s2p6s\rangle$, for example, contains all ns states with $n \geq 7$ but excluding $6s$.

$\|d\rangle$	L_{ab}	S_{ab}	e_c (Ry)	α (5.77)	α (22.07)	α 73.55)	$\bar{\sigma}$
$\|1s2s2p\rangle$	1	0	30.95	5.21×10^{-15}	3.66×10^{-14}	1.61×10^{-14}	2.02×10^{-21}
	1	1	30.95	1.48×10^{-14}	1.04×10^{-13}	4.56×10^{-14}	5.74×10^{-21}
$\|1s2s3p\rangle$	1	0	37.01	4.42×10^{-16}	6.74×10^{-15}	3.58×10^{-15}	4.09×10^{-22}
	1	1	37.01	1.26×10^{-15}	1.92×10^{-14}	1.02×10^{-14}	1.17×10^{-21}
$\|1s2p2\rangle$	0	0	31.79	2.93×10^{-15}	2.29×10^{-14}	1.03×10^{-14}	1.28×10^{-21}
	2	0	31.79	1.49×10^{-14}	1.17×10^{-13}	5.25×10^{-14}	6.51×10^{-21}
$\|1s2p3s\rangle$	1	0	37.34	1.66×10^{-15}	2.65×10^{-14}	1.42×10^{-14}	1.62×10^{-21}
	1	1	37.34	3.71×10^{-15}	5.91×10^{-14}	3.18×10^{-14}	3.61×10^{-21}
$\|1s2p3p\rangle$	0	0	37.54	6.42×10^{-16}	1.05×10^{-14}	5.67×10^{-15}	6.43×10^{-22}
	0	1	37.54	1.80×10^{-16}	2.94×10^{-15}	1.59×10^{-15}	1.80×10^{-22}
	2	0	37.54	3.28×10^{-15}	5.35×10^{-14}	2.89×10^{-14}	3.28×10^{-21}
	2	1	37.54	7.45×10^{-16}	1.22×10^{-14}	6.57×10^{-15}	7.45×10^{-22}
$\|1s2p3d\rangle$	1	0	37.73	1.11×10^{-16}	1.85×10^{-15}	1.01×10^{-15}	1.14×10^{-22}
	1	1	37.73	5.37×10^{-16}	8.98×10^{-15}	4.88×10^{-15}	5.52×10^{-22}
	3	0	37.73	3.23×10^{-15}	5.40×10^{-14}	2.93×10^{-14}	3.32×10^{-21}
	3	1	37.73	6.75×10^{-15}	1.13×10^{-13}	6.14×10^{-14}	6.95×10^{-21}
$\|1s2s4p\rangle$			38.93	4.92×10^{-16}	9.60×10^{-15}	5.42×10^{-15}	6.04×10^{-22}
$\|1s2p4s\rangle$			39.37	2.74×10^{-15}	5.65×10^{-14}	3.24×10^{-14}	3.59×10^{-21}
$\|1s2p4p\rangle$			39.45	2.96×10^{-15}	6.17×10^{-14}	3.54×10^{-14}	3.92×10^{-21}
$\|1s2p4d\rangle$			39.52	5.90×10^{-15}	1.24×10^{-13}	7.14×10^{-14}	7.90×10^{-21}
$\|1s2p4f\rangle$			39.55	8.25×10^{-16}	1.74×10^{-14}	1.00×10^{-14}	1.11×10^{-21}
$\|1s2p5s\rangle$			40.27	1.68×10^{-15}	3.89×10^{-14}	2.29×10^{-14}	2.51×10^{-21}
$\|1s2p5p\rangle$			40.31	2.24×10^{-15}	5.20×10^{-14}	3.07×10^{-14}	3.37×10^{-21}
$\|1s2p5d\rangle$			40.34	3.86×10^{-15}	9.02×10^{-14}	5.33×10^{-14}	5.84×10^{-21}
$\|1s2p5f\rangle$			40.36	5.87×10^{-16}	1.38×10^{-14}	8.13×10^{-15}	8.91×10^{-22}
$\|1s2p6s\rangle$			40.74	1.13×10^{-15}	2.78×10^{-14}	1.66×10^{-14}	1.81×10^{-21}
$\|1s2p6p\rangle$			40.77	1.85×10^{-15}	4.56×10^{-14}	2.73×10^{-14}	2.98×10^{-21}
$\|1s2p6d\rangle$			40.79	2.63×10^{-15}	6.50×10^{-14}	3.89×10^{-14}	4.25×10^{-21}
$\|1s2p6f\rangle$			40.80	3.89×10^{-16}	9.63×10^{-15}	5.77×10^{-15}	6.30×10^{-22}
Totals				8.77×10^{-14}	1.26×10^{-12}	6.82×10^{-13}	7.76×10^{-20}

Extrapolated from $\|d\rangle$	L_{ab}	S_{ab}	e_c (Ry)	Extrapolation values using scaling α (5.77)	α (22.07)	α (73.55)	$\bar{\sigma}$
$\|1s2s4p\rangle$	1	0	38.92	1.56×10^{-16}	3.64×10^{-15}	2.15×10^{-15}	2.36×10^{-22}
	1	1	38.92	4.44×10^{-16}	1.04×10^{-14}	6.14×10^{-15}	6.73×10^{-22}
$\|1s2p6s\rangle$	1	0	40.74	3.27×10^{-16}	9.03×10^{-15}	5.56×10^{-15}	6.01×10^{-22}
	1	1	40.74	7.52×10^{-16}	2.03×10^{-14}	1.24×10^{-14}	1.34×10^{-21}
$\|1s2p6p\rangle$	0	0	40.77	1.46×10^{-16}	4.05×10^{-15}	2.50×10^{-15}	2.70×10^{-22}
	0	1	40.77	1.13×10^{-17}	3.11×10^{-16}	1.91×10^{-16}	2.07×10^{-23}
	2	0	40.77	7.95×10^{-15}	2.16×10^{-13}	1.33×10^{-13}	1.44×10^{-20}
	2	1	40.77	2.22×10^{-16}	5.93×10^{-15}	3.62×10^{-15}	3.92×10^{-22}
$\|1s2p6d\rangle$	1	0	40.79	4.83×10^{-18}	1.33×10^{-16}	8.17×10^{-17}	8.84×10^{-24}
	1	1	40.79	4.09×10^{-17}	1.12×10^{-15}	6.85×10^{-16}	7.41×10^{-23}
	3	0	40.79	6.11×10^{-16}	1.69×10^{-14}	1.04×10^{-14}	1.12×10^{-21}
	3	1	40.79	1.52×10^{-15}	4.13×10^{-14}	2.53×10^{-14}	2.74×10^{-21}
$\|1s2p6f\rangle$	2	0	40.80	1.12×10^{-18}	3.01×10^{-17}	1.84×10^{-17}	2.00×10^{-24}
	2	1	40.80	1.61×10^{-18}	4.31×10^{-17}	2.63×10^{-17}	2.86×10^{-24}
	4	0	40.80	3.57×10^{-17}	9.87×10^{-16}	6.08×10^{-16}	6.57×10^{-23}
	4	1	40.80	1.24×10^{-16}	3.39×10^{-15}	2.08×10^{-15}	2.25×10^{-22}
Total extrapolations				1.24×10^{-14}	3.34×10^{-13}	2.05×10^{-13}	2.22×10^{-20}

TABLE IV. (*Continued*).

Extrapolated from $\|d\rangle$	L_{ab}	S_{ab}	e_c (Ry)	α (5.77)	Extrapolation values using scaling α (22.07)	α (73.55)	$\bar{\sigma}$
					Totals including extrapolation		
				α (5.77)	α (22.065)	α (73.551)	$\bar{\sigma}$
				1.00×10^{-13}	1.59×10^{-12}	8.87×10^{-13}	9.97×10^{-20}

the Fe ions.[10,11] It contains three electrons in the ion after the capture, so that, as compared to the H-like ions, some additional complications arise due to the presence of the $1s$ spectator electron. We present the details of our data in Table III for C^{4+} and in Table IV for O^{6+}. Figure 3 summarizes the rates for C^{4+} and O^{6+}, and compares with the earlier results.[12]

Three points should be specially noted. (i) The total rates are only slightly increased as we go from C to O, although the dominant stabilizing transition $A_r(2p\rightarrow1s)$ has increased by nearly a factor of 4 (the Z^4 scaling), while $A_a(d\rightarrow i)$ remained nearly constant. (ii) The HRS contribution is much less for the He-like ions, approximately 20–30% of the total, than that for the H-like ions, where the contribution was nearly 50% of the total. This is caused by the presence of the $1s$ spectator electron in the He-like ion case, which splits the $2s-2p$ degeneracy. Thus, for $n\geq n_m=5$ for C^{4+} and $n_m=7$ for O^{6+}, an extra Auger channel $1s2pnl\rightarrow1s2s+e'$ opens up, with a large Auger transition probability. This increases the total width of the state (d) and reduces the fluorescence yield and the rates by as much as a factor of 3 of the HRS contribution ($n\geq n_m$). We have also examined the effect of different coupling orders such as CSC within the LS coupling and compared with the APC adopted here. We found that the APC often gives smaller rates than that obtained by CSC for the even-parity intermediate states and larger rates for the odd-parity states. The total rates are almost always found to be unchanged, however, to within a few percent. In all cases, the individual rates in LS coupling are smaller than the values obtained in angular momentum average scheme.[1]

(ii) The configuration mixing effect was also considered for some of the dominant intermediate states of even and odd parities. For even-parity states the mixing generally increases the rates, while for odd states which are by far the dominant ones in the He-like ions, it decreases the rates. The overall effect of configuration mixing on the total rates is a change of less than 5%. It is therefore reasonable to conclude that the calculated DR rates for C^{4+} and O^{6+} have converged, with an approximate accuracy of ±5%. The recent work of Chen[12] is about 3–5 % lower than the rates obtained in this work.

(iii) The radiative cascade correction is found to affect some of the intermediate states d, but in most cases the effect is not very large mainly because of the dominance of the radiative transition $A_r(2p\rightarrow1s)$ in the total Γ_r. For example, in O^{6+} ($1s2p3d$, $L_{ab}=3$, $S_{ab}=0$), we have $\Gamma_r=1.01\times10^{12}$ sec^{-1}, $\Gamma_a=5.34\times10^{12}$ sec^{-1}, and $\sigma=3.23\times10^{-21}$ cm^2, where the cascade-corrected $\Gamma_r=7.95\times10^{11}$ sec^{-1}. This results in a reduction of the cross section by approximately 25%.

TABLE V. Fitting parameters for the DR rates, Eq. (6), for the four ions $C^{5+,4+}$ and $O^{7+,6+}$. The overall fit is at the ±5% level, which is well within the accuracy of the calculation.

	C^{5+}	O^{7+}	C^{4+}	O^{6+}
A (10^{-10} cm^3/s)	5.0	1.0	3.0	9.8
e_c (Ry)	24	45	18	36
B (Ry)	−2.0	−2.0	−1.5	−2.0

C. Empirical rate formula

A simple three-parameter fit is obtained for each ion of Z_c, using a form

$$\alpha^{\rm DR}_{\rm emp}(Z_c,Z,k_BT_e)$$
$$=A(k_BT_e)^{-3/2}\exp(-\bar{e}_c/k_BT_e)(1+B/k_BT_e)\,, \quad (6)$$

where the fitted parameters A, B, and $\bar{e}_c$ are given in Table V, k_BT_e and e_c are given in rydbergs, and A is in units of 10^{-10} cm^3/sec.

D. Metastable initial states capture

Recent high-resolution measurement of the DR cross sections for the initial metastable states by Andersen *et al.*[13] prompted a theoretical calculation of the cross sections for some of the low-lying intermediate states. Table VI summarizes the relevant energy levels and the calculated cross sections. Detailed comparison with experimental data is deferred until the uncertainty in the normalization of the metastable initial beam is clarified,[14] but the ratios between the peaks of the same Rydberg series seem to be consistent with the data.

IV. CONCLUSION

We presented the DR cross sections and rate coefficients for the four ions, $C^{4+,5+}$ and $O^{6+,7+}$. By comparing our result with the earlier calculations and by critically assessing the various approximations involved,

TABLE VI. DR cross sections for different metastable initial states of O are tabulated, together with the relevant energy values. S is the velocity-weighted average cross section.

$1s2s \rightarrow 1s2pnl$ Transition	Configuration	e_c (eV)	$\bar{\sigma}^{DR}$ (10^{-17} cm^2)	S (10^{-10} cm^3 eV/sec)
$^3S \rightarrow {}^1P$	$7s$	2.4	4.1	5.2
	$7p$	2.9	1.1	1.5
	$7d$	2.9	4.3	5.8
	$7f$	3.0	1.5	2.1
	$\geq 7g$	3.0	1.1	1.5
			12.0	16.1
$^3S \rightarrow {}^3P$	$9s$	1.4	0.001	0.001
	$9p$	1.6	0.060	0.062
	$\geq 9d$	1.6	0.001	0.001
			0.061	0.063
$^3P \rightarrow {}^1P$	$10s$	0.3	4.2	1.7
	$10p$	0.4	7.5	3.9
	$10d$	0.4	7.6	3.9
	$10f$	0.4	3.6	1.9
	$\geq 10g$	0.5	0.12	0.06
			23.0	11.4
$^1S \rightarrow {}^1P$	$11s$	0.9	18	14
	$11p$	1.0	29	23
	$11d$	1.0	30	24
	$11f$	1.0	71	58
	$11g$	1.0	98	79
	$11h$	1.0	109	89
	$\geq 11i$	1.0	326	265
			680	552
		$\Delta e_c = 0.01$ Ry		

we conclude that the rates given here are reliable to approximately $\pm 5\%$ for the H-like C^{5+} and O^{7+}, and $\pm 5\%$ also for the He-like C^{4+} and O^{6+}. It is somewhat surprising that the simple single-configuration calculation of this paper agrees so well with the earlier more elaborate calculation of Ref. 12 for the He-like ions.

Extensions of the similar considerations to other charged states of C and O are underway, and the result will be reported on elsewhere. In view of the important role played by the HRS in these ions, the effect of plasma field and density should be sizable and must be incorporated into the final rates.

ACKNOWLEDGMENTS

The work reported here was supported in part by a U.S. Department of Energy grant. We thank Dr. L. Andersen, Dr. P. Hvelplund, and Dr. H. Knudsen for sending us their result prior to publication.

[1]Y. Hahn, Adv. Atom. Molec. Phys. **21**, 123 (1985).
[2]Y. Hahn, Phys. Scr. **T28**, 25 (1989).
[3]K. LaGattuta and Y. Hahn, Phys. Lett. A **84**, 468 (1981).
[4]R. D. Cowan, *Theory of Atomic Structure and Spectra* (University of California Press, Berkeley, 1981); and private communications.
[5]K. R. Karim and C. P. Bhalla, Phys. Rev. A **37**, 2599 (1988).
[6]T. Fujimito *et al.*, Nagoya University Report No. IPPJ-AM-23 1982 (unpublished).
[7]I. Nasser and Y. Hahn, J. Quant. Spectrosc. Radiat. Transfer **29**, 1 (1983).
[8]S. Younger, J. Quant. Spectrosc. Radiat. Transfer **29**, 67 (1983).
[9]F. Bely-Dubau *et al.*, Phys. Rev. A **26**, 3459 (1982).
[10]J. Dubau *et al.*, Mon. Not. Astro. Soc. **195**, 705 (1981).
[11]M. Bitter *et al.*, Phys. Rev. Lett. **43**, 129 (1979).
[12]M. H. Chen, Phys. Rev. A **38**, 6430 (1988).
[13]L. Andersen, P. Hvelplund, H. Knudsen, and P. Kvistgaad, Phys. Rev. Lett. **62**, 2656 (1989).
[14]Y. Hahn and R. Bellantone, Phys. Rev. A (to be published).